

Kardar-Parisi-Zhang growth of amorphous silicon on Si/SiO₂

M. Lütt,* J. P. Schlomka, M. Tolan, J. Stettner, O. H. Seeck, and W. Press

Institut für Experimentalphysik, Christian-Albrechts-Universität Kiel, Olshausenstraße 40-60, 24098 Kiel, Germany

(Received 8 April 1996; revised manuscript received 6 September 1996)

Amorphous silicon films with thicknesses ranging from about 20 Å to 2000 Å were evaporated onto silicon substrates. The surface and interfaces were then investigated by specular and diffuse x-ray scattering experiments in the region of total external reflection. A model of self-affine interfaces was used for the refinement. The rms roughness σ and the in-plane correlation length ξ vs film thickness follow power laws with exponents of $\beta=0.1\pm0.05$ and $1/z=0.6\pm0.2$, and the average Hurst parameter is $h=0.23\pm0.05$. The resulting parameters are compatible with growth models based on the Kardar-Parisi-Zhang equation.
[S0163-1829(97)01531-2]

I. INTRODUCTION

The growth of artificial thin films and layer systems is an important technique used in modern industrial applications, e.g., microelectronics. One crucial factor is the inevitable interface and surface roughness occurring during layer growth. In order to avoid unnecessary rough interfaces and surfaces, one has to understand the physical processes involved. This paper aims at an experimental proof for layer growth described by the so-called Kardar-Parisi-Zhang (KPZ) equation.¹ To achieve this, amorphous silicon layers were investigated using x-ray reflectometry and diffuse scattering.

X-ray reflectometry is one of the commonly used methods to monitor surface roughness. By this technique, thicknesses and densities of the grown films and their interfacial roughness amplitudes can be obtained.²⁻⁴ However, due to the fact that specular reflectivity results in a wave-vector transfer perpendicular to the surface (the incident angle equals the exit angle), only information about the sample structure in that direction—the electron density profile perpendicular to the surface averaged over a large surface region—can be obtained. In order to obtain information about the mesoscopic in-plane interface structure, one has also to analyze the diffusely scattered intensity (the intensity scattered in other directions than the specular). The theory of diffuse scattering based on the distorted-wave Born approximation (DWBA) (Ref. 5) has been worked out in detail over the last years.⁶⁻¹⁰ It also was shown that the DWBA can be applied to real systems and parameters describing the out-of plane and in-plane structures of the interfaces can be obtained (see, e.g., Refs. 9 and 11–15).

In this paper we will show that not only specular and diffuse scattering can be refined using the above-mentioned theory but also that functional dependences of the interface parameters vs the layer thickness can be derived from x-ray diffraction at grazing angles. This enables us to assign the growth process to a specific universality class which then, by comparison with theoretical predictions, provides information about the microscopic processes during growth, e.g., surface relaxation or surface diffusion.

Previously in many cases a power-law behavior of the rms roughness vs thickness was found (for an overview, see

Ref. 16). However, the exponents vary from case to case, and seem to be very sensitive to the particular material and growth conditions, e.g., deposition methods, growth rates, and temperatures. A large body of work was done on the growth of metals. For example Thompson *et al.*¹⁷ investigated the growth of silver films on silicon by x-ray reflectivity techniques. They obtained a power law for the rms roughness $\sigma \propto t^{0.26}$, which is consistent with growth described by the KPZ equation (see Sec. II B). However, that theory also predicts a specific value for the so-called Hurst-parameter h (see Sec. II A) of $h=0.18-0.40$. Rather than constraining the parameters and using the full theory in the analysis, the authors went to a single interface approximation yielding $h=0.7$.

On the other hand, in W/C multilayers, a logarithmic behavior of the in-plane correlation length (see Sec. II A) was found¹⁸ which corresponds to the limit $h \rightarrow 0$ (Edward-Wilkinson-like growth type¹⁹). Several authors report scanning-tunneling-microscopy measurements on silicon surfaces. Wu *et al.*²⁰ investigated molecular-beam-epitaxy (MBE) growth of Si on Si(001) at $\sim 350^\circ\text{C}$, and found $\sigma \propto t^{0.29}$ and $h=0.45$. For a similar system Hegeman *et al.*²¹ published $h=0.68$ in the island growth regime (substrate temperature $\sim 300^\circ\text{C}$) but found a nonalgebraic behavior in the step-flow mode (temperature above 600°C). Yoshinobu *et al.*²² measured the Si(100) surface produced by HF-etching to remove the oxide. They found values of $h=0.3-0.5$.

In our experiment the deposition was done at room temperature with a much higher rate than used for MBE, and therefore amorphous layers are produced. The theory of single crystal growth (e.g., step flow) is not applicable, and it is not surprising that the exponents obtained in this work are different from the above-mentioned ones. To our knowledge no work on the growth of surface roughness of thin amorphous silicon layers has yet been published. Furthermore, the previous x-ray works lack a complete data analysis using a full dynamical scattering theory. To fill this gap we derived growth exponents from our data by applying a complete x-ray scattering theory, based on the DWBA for layer systems,^{8,9} which was successfully used to explain x-ray data from many systems before.¹²⁻¹⁵

The paper is structured as follows. In Sec. II the descrip-

tion of interfaces via correlation functions is introduced, and the KPZ theory of film growth is described briefly. Section III discusses the experimental conditions: the sample preparation and the x-ray experiments. The results and the accuracy of the obtained exponents are discussed in Sec. IV. Conclusions and an outlook are given in Sec. V.

II. THEORY

A. Correlation functions

Interfaces can be statistically described by an autocorrelation function $C_j(\mathbf{R})$.^{16,23} For isotropic surfaces produced by random deposition or other statistical growth processes, a description in terms of self-similarity²⁴ is often used. One correlation function describing such surfaces is given by⁶

$$C_j(R) = \sigma_j^2 e^{-(R/\xi_j)^{2h_j}}, \quad (1)$$

with the cutoff (correlation) length ξ_j and the Hurst parameter h_j of the j th interface.^{16,23} The quantity ξ_j describes the maximum lateral length scale on which in-plane roughness correlations persist. Only for $R < \xi_j$ the surface shows self-affine scaling behavior. The Hurst parameter h_j defines the fractal dimension $D_j = 3 - h_j$ (Ref. 24) of the interface and is therefore restricted to the region $0 < h_j \leq 1$. Small values of h_j produce extremely jagged surfaces, while values of $h_j \approx 1$ lead to interfaces with smooth hills and valleys.¹² σ_j is the root-mean-square (rms) roughness of interface j .

In many cases correlations between interfaces of a layer system are present because the interface shape of an underlying layer is transferred to upper layers due to layer by layer growth on an atomic or molecular scale. The correlations between different layers j and k are described by the cross-correlation function $C_{jk}(\mathbf{R})$. In our data analysis $C_{jk}(\mathbf{R})$ is given by¹⁴

$$C_{jk}(\mathbf{R}) = \mathcal{F}^{-1} \{ \sqrt{L_j(\mathbf{q}_r) \cdot L_k(\mathbf{q}_r)} \cdot e^{-d_{jk}/\xi_{\perp,jk}} \}. \quad (2)$$

$L_j(\mathbf{q}_r)$ denotes the Fourier transform of the autocorrelation function of interface j , d_{jk} is the distance between the interfaces, i.e., the layer thickness. \mathcal{F}^{-1} is the Fourier back-transformation. The length $\xi_{\perp,jk}$ can be understood as a vertical distance over which the correlations between layers j and k are damped by a factor of $1/e$. No correlations are present in the case $\xi_{\perp,jk} = 0$, and nearly perfect correlation means that $\xi_{\perp,jk}$ is much larger than the layer thicknesses. In this case additional oscillations occur in off-specular q_z scans (for details, see Ref. 9).

B. Growth models

The theory of growth and the shape of the resulting surfaces has been studied intensively by computer simulations and calculations based on various growth equations (for reviews, see Refs. 16, 23, and 25). In most cases one starts with a flat surface, and during the deposition the rms roughness σ and the in-plane correlation length ξ grow according to the following power laws:

$$\sigma \sim t^\beta, \quad (3)$$

$$\xi \sim t^{1/z}. \quad (4)$$

t represents the total growth time which is proportional to the layer thickness for a constant deposition rate. The resulting surface exhibits self-affine properties given by Eq. (1) and the so-called *Family-Vicsek scaling relation*^{26,16} is valid. From that scaling relation it can be calculated that the exponents β and $1/z$ are related to the Hurst-exponent h via

$$h = \beta z. \quad (5)$$

This means that in our experiment, where we can determine the three values h , β , and ξ independently, the validity of Eq. (5) is necessary to identify a growth process of the above type. We should note here that due to finite-size effects neither σ nor ξ will grow to infinity as the growth continues, but will reach saturate values.

One description of growth processes that takes into account a random deposition and a limited relaxation of particles²⁷ on the surface is given by the well-known KPZ equation, first introduced by Kardar, Parisi, and Zhang.¹

$$\frac{\partial s(\mathbf{r}, t)}{\partial t} = \nu \nabla^2 s + \frac{\lambda}{2} (\nabla s)^2 + \eta(\mathbf{r}, t). \quad (6)$$

$s(\mathbf{r}, t)$ is the thickness of deposited material at a lateral position \mathbf{r} at time t . The first term on the right-hand side describes relaxation (redistribution of material) due to surface tension ν , the second term describes the dependence of growth on local surface inclines (lateral growth), and $\eta(\mathbf{r}, t)$ is a noise term accounting for the deposition of material (for details see Refs. 1 and 16). The invariance of Eq. (6) under rescaling leads to the second relation between the growth parameters which has to be fulfilled:²⁵

$$h + z = 2. \quad (7)$$

An analytical solution of the KPZ equation was only found for the one-dimensional case.²⁸ However, by large-scale computer simulations and numerical integrations, values for the growth exponent β and the Hurst parameter h were obtained also for the here relevant two-dimensional case [$\beta = 0.10$ – 0.25 and $h = 0.18$ – 0.40 (Refs. 16, 23, and 25)].

Growth processes belonging to different universality classes exhibit different values for those exponents and, in some cases, also different scaling relations. For example, if one neglects the nonlinear term in the KPZ equation (the term accounting for lateral growth) which leads to the Edwards-Wilkinson (EW) model,¹⁹ the exponents turn out to be $h = \beta = 0$. In this case the in-plane correlation decays logarithmically. Another example is the inclusion of surface diffusion (a crucial factor in MBE processes) which leads to $h = 1$ and $\beta = \frac{1}{4}$ for the simplest case (replacing the surface tension term in the EW equation by a surface curvature term $\propto \nabla^4 s$) and to $h = \frac{2}{3}$ and $\beta = \frac{1}{5}$ for a more realistic, nonlinear model.¹⁶

We see from these examples that the exponents take on distinct values depending on the dominating physical processes. By determining h , β , and $1/z$, particular models are favored to explain the growth process, and others can be ruled out. Therefore, knowledge about the microscopic deposition process is gained.

To summarize, growth described by the KPZ equation can be identified by fulfilling following three conditions: (i) $h = \beta z$. (ii) $h + z = 2$. (iii) $\beta = 0.10$ – 0.25 and $h = 0.18$ – 0.40 .

The aim of the present study is to show that for the system SiO_2/Si , these conditions are fulfilled, and therefore this system can be identified as KPZ-like.

III. SAMPLE PREPARATION, EXPERIMENTAL SETUP AND MEASUREMENTS

The deposition of the silicon layers was done onto cleaned silicon (100) substrates at room temperature using a commercial evaporation system (Balzers BAK550). A set of six samples was prepared with nominal thicknesses of 20, 70, 200, 400, 800, and 2000 Å. Growth under these conditions results in amorphous Si layers, where a wide range of densities had been found.^{29–32} The samples were not held in vacuum after the deposition, and therefore a thin top-oxide layer cannot be avoided.

The x-ray experiments were performed using a 12-kW rotating anode with Copper target and a two-circle diffractometer with NaI scintillation detector.³³ Ge(111) crystals were used as monochromator and analyzer. For each sample the reflectivity and six diffuse scans (rocking scans, detector scans, and one longitudinal diffuse scan) were performed. A rocking scan is done by placing the detector at a fixed angular position Φ and rotating the sample. The incident angle α_i and exit angle α_f fulfill the condition $\alpha_i + \alpha_f = \Phi$. For small detector angles a rocking scan is equivalent to a q_x scan at a constant q_z . q_x and q_z are the wave-vector transfers in and perpendicular to the surface.¹² For a detector scan the sample is fixed at a constant incident angle α_i , and the detector angle Φ is varied. In reciprocal space the track of this scan is a circle. Finally, the longitudinal diffuse scan is performed by rotating the sample and the detector so that $\alpha_i = \Phi/2 + \delta$, where δ is a fixed offset angle. Figures 1, 2, and 3 show the measurement and refinement of the reflectivity, one rocking scan, and one detector scan for each sample as examples. Note that the refinement for each sample was carried out using the whole dataset of reflectivity and diffuse scans as described in Refs. 12–14.

In our opinion only this procedure stabilizes the physical results. Flat interfaces are mainly visible in the reflectivity curve, whereas rough interfaces produce large diffuse scattering and can be seen in off-specular scans.

IV. RESULTS AND DISCUSSION

Table I shows the resulting parameters of the simultaneous refinement of the reflectivity and six diffuse scans for each sample. In all cases a three-layer model (the substrate with an oxide, the evaporated silicon layer, and a top oxide layer) leads to a sufficient quality of the fit. Deviations between measurement and fit are mainly present in the reflectivity curves of the thin films. This is caused by the fact that the simple model does not reflect all details of the density profile. However, the diffuse scans which contain information about the rough interface (the surface of the grown layer which we are interested in) are well explained by the theory. The increased intensity in the low-angle region of the detector scans (Fig. 3) are an experimental artifact due to the primary beam.

The scattering contribution of the substrate/oxide interface is weak due to the small contrast between substrate and

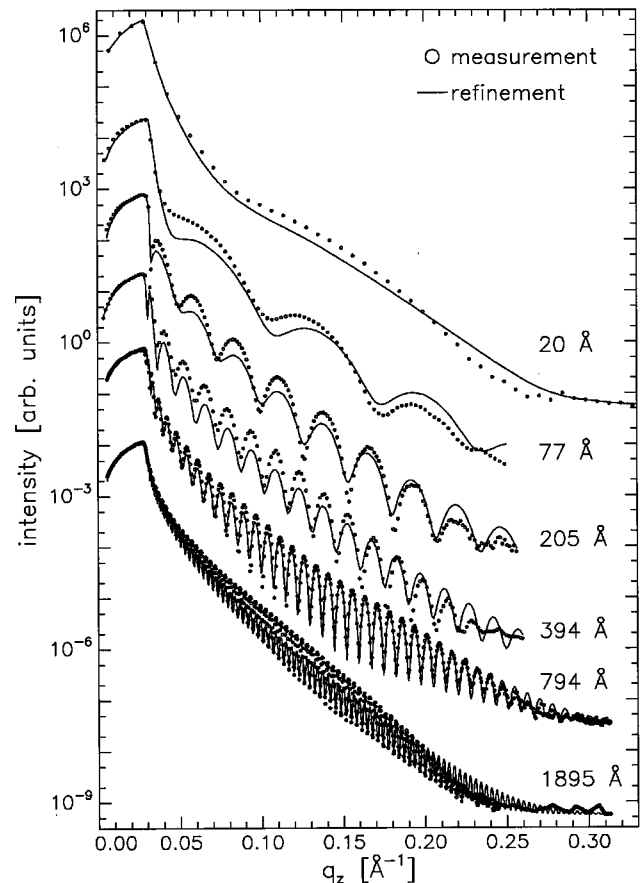


FIG. 1. Measurement and refinement of the specular reflectivity for the six samples. The refinement was done with a dataset containing the reflectivity and six diffuse scans for each sample. Therefore not perfect fits were obtained.

oxide which results in a large uncertainty of the substrate parameters. The rms-roughnesses are between 5 and 10 Å, the in-plane correlation lengths are relatively short (≈ 1000 Å). The Hurst parameter can hardly be determined. It is certainly larger than 0.1, because otherwise peaking diffuse scattering would occur which cannot be seen in our measurements.

The oxide layer that covers the substrate has an electron density of approximately 80–90 % of the Si-substrate value. The thickness ranges from 10 to 15 Å, and the rms roughness lies in the same region. The parameters describing the in-plane structure of the lower oxide interface (ξ, h) can also be determined with large uncertainty. The Hurst parameter is larger than 0.2, and the correlation length is longer than that for the substrate/oxide interface.

To summarize the influence of the two lower interfaces, it can be stated that the contribution to the diffuse scattering is negligible, whereas there is some influence on the calculated specular reflectivity if the rms roughness parameters are altered violently. The evaporated amorphous Si layers exhibit densities of 80–90 % of single crystals, which is consistent with values previously found by us¹² and others.^{30–32}

We now concentrate on the upper interfaces and their properties that are produced by the growth process. Two very different types of interfaces seem to be present: The very rough surface of the grown Si layer with a large correlation length and a smoother oxide layer on top with a short

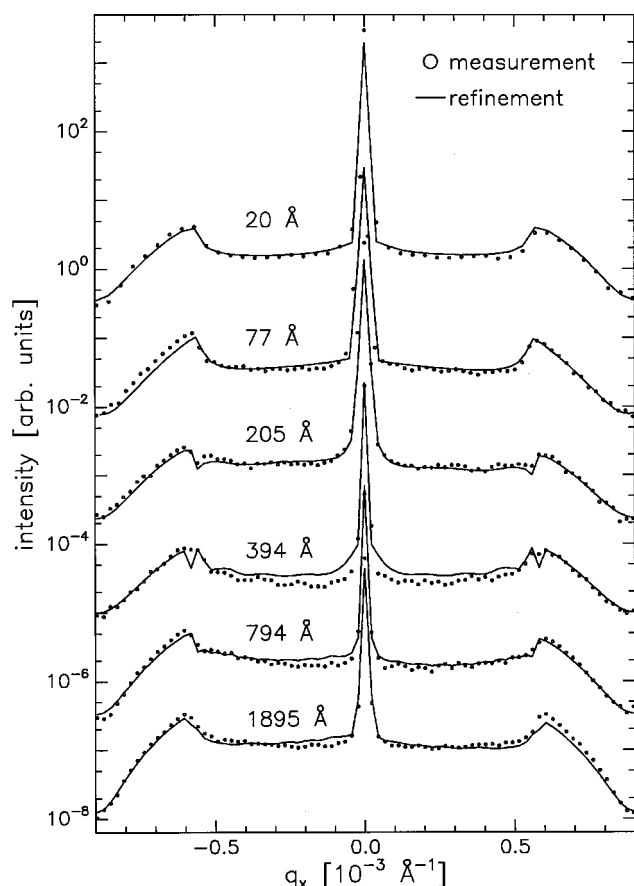


FIG. 2. Measurement and refinement of one rocking scan at a detector angle of 1.2° ($q_z = 0.17 \text{ \AA}^{-1}$). A rocking scan is performed by placing the detector at a fixed angle and rotating the sample. For small detector angles this is equivalent to a q_x scan (q_x is the in-plane wave-vector transfer) at a constant q_z (q_z is the wave-vector transfer perpendicular to the surface).

correlation length. In an alternative data analysis, we tried to explain the scattering with just one layer (amorphous silicon) or two layers (SiO_2/Si on the Si substrate). This clearly failed, so that the three-layer model had to be applied. Unfortunately a large scattering contribution is in fact produced by the oxide/air interface due to the large density contrast. However, there clearly is an additional contribution from the Si-layer/ SiO_2 interface, and the parameters describing both interfaces were obtained by our data analysis with the given accuracy.

In the refinement the large roughness of the Si-layer/ SiO_2 interface leads to the fact that this interface hardly contributes to the specular reflectivity, but shows strong diffuse scattering even though the contrast to the top oxide is small. The top oxide itself provides the main contribution to the reflectivity, and approximately the same amount of diffuse scattering as the very rough Si interface. This behavior, together with the fact that the top oxide is rather thin (10–15 Å), leads to the conjecture that the electron-density profile of the sample surface cannot be described by two separate interfaces but rather by one non-Gaussian-shaped density profile with two different parts: a very rough, smeared-out profile, and rather abrupt variations (steps), e.g., at the SiO_2/air termination of the interface. Whereas the reflectivity of arbitrary shaped interfaces can be calculated using recursive ma-

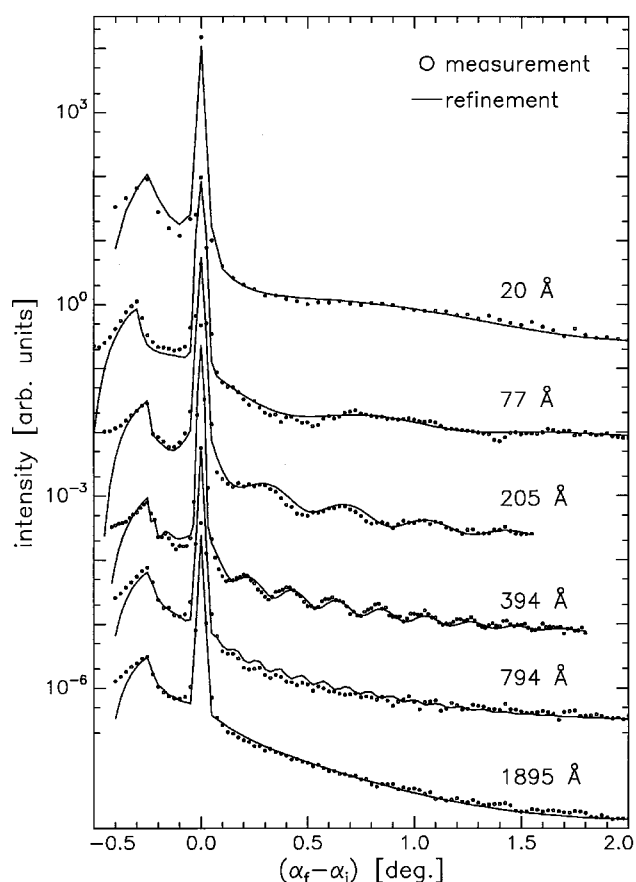


FIG. 3. Measurement and refinement of one detector scan at an incident angle of 0.45° (for the 77-Å film the incident angle is 0.5°). A detector scan is performed by rotating the detector at a fixed angle of incidence.

trix methods,^{2,3} it is extremely difficult to calculate the diffuse scattering of systems of the above type.¹⁰ Therefore we model this broad Si/ SiO_2 /air interface by two single interfaces, bearing in mind that the parameters (d and σ) of the upper interface now do not have the meaning of a layer thickness and a rms roughness. For example, a roughness of $\sigma \approx 10 \text{ \AA}$ of the oxide/air interface does *not* mean that the oxide layer is able to damp the 40-Å roughness of the Si/ SiO_2 interface underneath. It means that the Si/ SiO_2 /air interface has a particular shape (see, as an example, Fig. 4). Note furthermore that both interfaces have totally different lateral length scales (see ξ values in Table I), also indicating that the topmost oxide layer was not grown as a conformal uniform thin layer.

In the series of films, the $d = 20 \text{ \AA}$ thick film is more problematic. The thickness of this film is smaller than the rms roughness of the Si/ SiO_2 interface. Therefore the density profiles of three interfaces interfere. Again one should bear in mind that the real situation is better described by one density profile rather than three interfaces as used in our calculations. The three-interface model can be interpreted as a parametrization of this above-mentioned single-density profile.

If the diffuse part of the scattered intensity is neglected and only the specular reflectivity is refined, a rather perfect fit but very different roughnesses are obtained (roughnesses of 6–15 Å are obtained following a power law with β

TABLE I. Results of the simultaneous refinement of reflectivity and diffuse scattering for the set of six samples. Braced values could not be refined, and were kept constant.

| Sample | | Substrate | SiO ₂ layer | Si layer | SiO ₂ layer |
|--------------|--------------------------|---------------------|--------------------------------|-------------------------------|------------------------|
| 20-Å Si | $\delta \times 10^6$ | | $6.6^{+0.3}_{-0.5}$ | 6.3 ± 0.1 | 5.4 ± 0.2 |
| | $\sigma/\text{\AA}$ | 11^{+5}_{-3} | 4^{+5}_{-2} | 41 ± 5 | 8.8 ± 1 |
| | $d/\text{\AA}$ | | 10 ± 4 | 20 ± 5 | 14 ± 5 |
| | $\xi/\text{\AA}$ | ≤ 200 | $100 \dots 50\,000$ | $5500^{+10\,000}_{-4000}$ | ≤ 100 |
| | h | 0.7 ± 0.3 | $0.8^{+0.2}_{-0.5}$ | 0.10 ± 0.05 | $0.26^{+0.05}_{-0.03}$ |
| | $\xi_{\perp}/\text{\AA}$ | | | ≥ 100 | |
| 70-Å Si | $\delta \times 10^6$ | | 6.6 ± 0.3 | 6.0 ± 0.1 | 5.1 ± 0.1 |
| | $\sigma/\text{\AA}$ | 3^{+3}_{-2} | ≤ 8 | 38 ± 5 | 8.0 ± 1 |
| | $d/\text{\AA}$ | | 13 ± 3 | 77 ± 5 | 8 ± 3 |
| | $\xi/\text{\AA}$ | ≤ 2000 | $100 \dots 100\,000$ | $14000^{+10\,000}_{-5000}$ | ≤ 100 |
| | h | 0.6 ± 0.4 | 0.6 ± 0.4 | 0.25 ± 0.05 | 0.35 ± 0.1 |
| | $\xi_{\perp}/\text{\AA}$ | | | ≥ 200 | |
| 200-Å Si | $\delta \times 10^6$ | | 6.3 ± 0.2 | 6.7 ± 0.05 | 6.3 ± 0.1 |
| | $\sigma/\text{\AA}$ | 6^{+3}_{-2} | 12 ± 5 | 55 ± 5 | 10.6 ± 1 |
| | $d/\text{\AA}$ | | 13 ± 4 | 205 ± 5 | 12 ± 3 |
| | $\xi/\text{\AA}$ | 300^{+500}_{-200} | $57000^{+30\,000}_{-20\,000}$ | $18000^{+20\,000}_{-10\,000}$ | ≤ 100 |
| | h | 0.6 ± 0.4 | $0.9^{+0.1}_{-0.5}$ | 0.33 ± 0.1 | 0.19 ± 0.05 |
| | $\xi_{\perp}/\text{\AA}$ | | | 400^{+1000}_{-100} | |
| 400-Å Si | $\delta \times 10^6$ | | 5.8 ± 0.2 | 6.1 ± 0.1 | 5.6 ± 0.1 |
| | $\sigma/\text{\AA}$ | 9 ± 2 | 16^{+10}_{-5} | 50 ± 5 | 10.3 ± 1 |
| | $d/\text{\AA}$ | | 12 ± 10 | 394 ± 5 | 12 ± 4 |
| | $\xi/\text{\AA}$ | ≤ 100 | $50000^{+100\,000}_{-30\,000}$ | $37000^{+50\,000}_{-25\,000}$ | ≤ 100 |
| | h | 0.6 ± 0.4 | $0.9^{+0.1}_{-0.7}$ | 0.23 ± 0.1 | 0.22 ± 0.05 |
| | $\xi_{\perp}/\text{\AA}$ | | | ≥ 400 | |
| 800-Å Si | $\delta \times 10^6$ | | 5.8 ± 0.2 | 6.9 ± 0.1 | 5.3 ± 0.2 |
| | $\sigma/\text{\AA}$ | 8^{+3}_{-2} | 9 ± 3 | 52 ± 5 | 11.2 ± 1 |
| | $d/\text{\AA}$ | | 14 ± 5 | 794 ± 5 | 12^{+4}_{-3} |
| | $\xi/\text{\AA}$ | ≤ 100 | $49000^{+150\,000}_{-20\,000}$ | $55000^{+50\,000}_{-40\,000}$ | 400 ± 100 |
| | h | ≥ 0.1 | ≥ 0.2 | 0.23 ± 0.1 | 0.7 ± 0.3 |
| | $\xi_{\perp}/\text{\AA}$ | | | ≥ 2000 | |
| 2000-Å Si | $\delta \times 10^6$ | | 5.9 ± 0.3 | 6.5 ± 0.05 | 6.1 ± 0.05 |
| | $\sigma/\text{\AA}$ | 11 ± 2 | 11^{+10}_{-2} | 55 ± 5 | 11.5 ± 0.5 |
| | $d/\text{\AA}$ | | 12^{+5}_{-2} | 1895 ± 5 | 14^{+5}_{-3} |
| | $\xi/\text{\AA}$ | ≤ 100 | 700^{+1500}_{-600} | $66000^{+50\,000}_{-40\,000}$ | ≤ 100 |
| | h | ≥ 0.2 | (0.5) | 0.26 ± 0.1 | 0.23 ± 0.03 |
| | $\xi_{\perp}/\text{\AA}$ | | | (0) | |

$=0.2$). This clearly shows that in a complete data analysis the diffuse scattering has to be taken into account. Generally in a layer stack consisting of both rough and smooth interfaces, smooth layers may be identified by their specular reflectivity signal which “hides” the contributions of the rough layers. The situation is opposite in the case of diffuse scattering: Here the rough layers lead to strong scattering and hide the smooth interfaces. This fact suggests that taking into account the diffuse scattering may be of decisive importance even if only parameters like rms roughnesses and layer thicknesses are of interest.

Figure 5 shows a double logarithmic plot of the rms roughness σ of the Si-layer/SiO₂ interface vs Si thickness t . Fitting a straight line, the growth exponent $\beta=0.1 \pm 0.05$ can be obtained. A similar behavior was found for the in-

plane correlation length ξ with an exponent $1/z=0.6 \pm 0.2$ (Fig. 6). The value for ξ grows from 5500 Å (20-Å film) to 66 000 Å (2000-Å film). Such large values can only be obtained if the coherently illuminated area on the sample is still larger than ξ . This is the case in our experiment which clearly had been proved for this particular x-ray source and setup.³⁴ The Hurst parameters of that interface show no significant tendency, and the average value is $h=0.23 \pm 0.05$.

A crucial test for the plausibility of the resulting parameters are the scaling relations Eqs. (5) and (7). From $\beta=0.1$ and $1/z=0.6$ we calculate, applying Eq. (5) $h=0.17$ which is consistent with $h=0.23$ as obtained from the experiment within errors.

Comparing the above fit results with growth models we find that the resulting average Hurst parameter of $h=0.23$ is

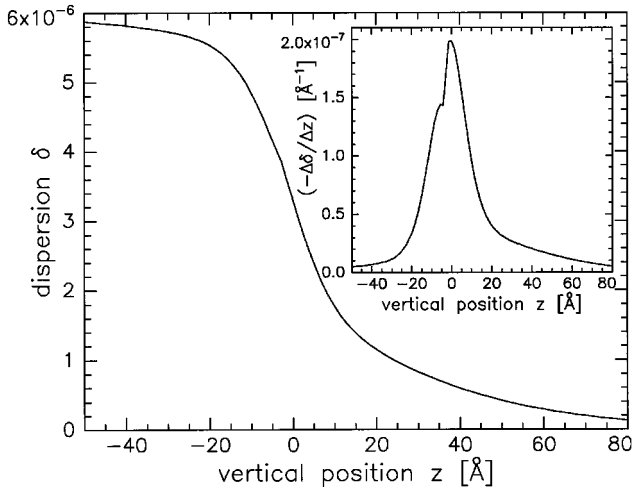


FIG. 4. Reconstruction of the dispersion profile from the refined parameters of Table I for the surface of the 77-Å film. The inset shows the derivative $-\Delta\delta/\Delta z$ which is equivalent to the roughness probability distribution. The two contributions from the rough Si layer/SiO₂ interface and the smoother SiO₂/air interface can be distinguished.

in accordance with KPZ-like models as described in Sec. II B and Refs. 1 and 16. Also, the rms roughness growth exponent $\beta=0.1$ and the exponent for the growth of the lateral correlation length $1/z=0.6$ are compatible with values predicted by those models. Furthermore also the second scaling relation given by Eq. (7) is almost perfectly fulfilled (our data: $h+z=1.98\approx 2$).

We can definitively rule out a logarithmic correlation function ($h\rightarrow 0$) as found in W/C multilayers.¹⁸ This means that lateral growth cannot be neglected, and that relaxation during deposition is present. We can also rule out significant surface diffusion which would lead to larger values for the Hurst parameter (see Sec. II B). Also the scaling relation Eq. (7) would not be valid in that case.

The error bars in Table I are obtained by manually changing the fit parameters until a significant deviation from the best fit occurs. It is obvious that the uncertainty is rather large, which is caused by the following reasons:

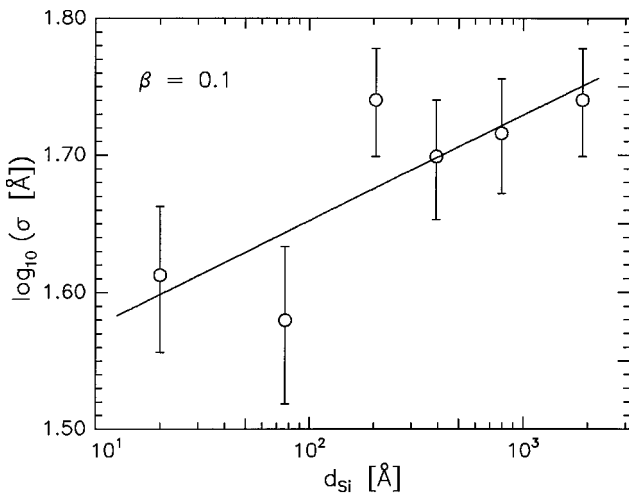


FIG. 5. Interface roughness σ_j of the Si-layer/SiO₂ interface vs film thickness.

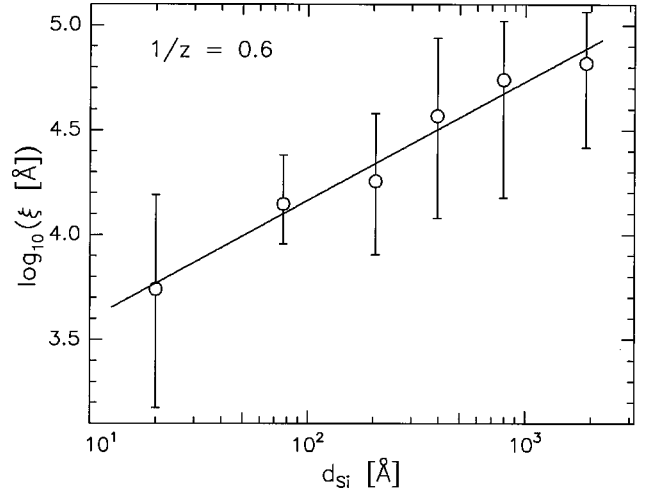


FIG. 6. In-plane correlation length ξ_j of the Si layer/SiO₂ interface vs film thickness.

(i) The maximum scattering contrast is given by the SiO₂/air interface. Therefore the influence of the most important Si-layer/SiO₂ interface is suppressed but still detectable.

(ii) Due to the limited in-plane wave-vector transfer and the resolution of the scattering experiment, the lateral length scales that can be resolved are limited to $\sim 100\text{--}100\,000$ Å. If the correlation length reaches either one of these limits, the uncertainty becomes very large. The Si-layer/SiO₂-interface correlation length grows to the upper limit which explains the large uncertainty for ξ .

However, the uncertainty is small enough to rule out certain growth models. The obtained values agree with simulations using a KPZ model, and they fulfill the scaling relations Eqs. (5) and (7). From that we can conclude that the growth process is most likely of the KPZ type.

Finally we want to discuss the influence of the initial substrate roughness on the growth process of our system. We found that the vertical correlation length ξ_{\perp} is always much larger than the thickness of the grown layers.³⁵ This means that the interfaces are almost perfectly correlated (see Sec. II A) and the substrate roughness does indeed influence the growth process. However, the roughness of the grown Si layer—the interface we are mainly interested in—is much larger than the substrate roughness (see Table I), which leads to the conclusion that the main contribution to the roughness is caused by the growth process itself and not just by the replication of the substrate roughness. Other authors¹⁷ take the substrate contour into account by decomposing the experimentally determined σ^2 :

$$\sigma^2 = \sigma_{\text{substrate}}^2 + \sigma_{\text{growth}}^2. \quad (8)$$

In our experiment this means that the substrate roughness can be totally neglected. A more sophisticated approach³⁶ predicts a decaying influence of the substrate roughness with the layer thickness following

$$\sigma^2 = \sigma_{\text{substrate}}^2 \left(\frac{t_0}{t_0 + t} \right)^{2/z} + \left(\frac{t}{t_1} \right)^{2\beta}. \quad (9)$$

t_0 and t_1 are constants,³⁷ and β and $1/z$ are defined as described in Sec. II B. However, our measurements show that

in the system Si/SiO₂/amorphous Si, the growth process strongly dominates the roughness. Note that this does not mean that conformal roughness as described in Sec. II A is absent.

V. SUMMARY AND OUTLOOK

We have shown, from specular and diffuse x-ray scattering experiments, that parameters describing the interfaces of amorphous Si on Si can be derived. The evolution of the rms

roughness and the in-plane correlation length of the upper film surface follow power laws as a function of the film thickness with exponents $\beta = 0.1 \pm 0.05$ and $1/z = 0.6 \pm 0.2$. The Hurst parameter that can also be derived from the experiment has an average value of $h = 0.23 \pm 0.05$. The comparison of these three parameters with growth models show that amorphous Si on Si is an almost perfect example for nonequilibrium growth as described by the KPZ theory.¹ In future work *in situ* STM investigations together with x-ray-diffraction measurements will reveal more accurate results.

-
- *Present address: Manuel Lujan, Jr., Neutron Scattering Center, Los Alamos National Laboratory, Los Alamos, New Mexico 87545.
- ¹M. Kardar, G. Parisi, and Y.-C. Zhang, Phys. Rev. Lett. **56**, 889 (1986).
 - ²F. Abelès, Ann. Phys. (Paris) **5**, 596 (1950).
 - ³L. G. Parrat, Phys. Rev. **95**, 359 (1954).
 - ⁴J. Lekner, *Theory of Reflection* (Nijhoff, Dordrecht, 1987).
 - ⁵G. H. Vineyard, Phys. Rev. B **26**, 4146 (1982).
 - ⁶S. K. Sinha, E. B. Sirota, S. Garoff, and H. B. Stanley, Phys. Rev. B **38**, 2297 (1988).
 - ⁷R. Pynn, Phys. Rev. B **45**, 602 (1992).
 - ⁸V. Holý, J. Kuběna, I. Ohlídal, K. Lischka, and W. Plotz, Phys. Rev. B **47**, 15 896 (1993).
 - ⁹V. Holý and T. Baumbach, Phys. Rev. B **49**, 10 668 (1994).
 - ¹⁰S. Dietrich and A. Haase, Phys. Rep. **260**, 1 (1995).
 - ¹¹D. Bahr, W. Press, R. Jevasinski, and S. Mantl, Phys. Rev. B **47**, 4385 (1993).
 - ¹²J.-P. Schlomka, M. Tolan, L. Schwalowsky, O. H. Seeck, J. Stettner, and W. Press, Phys. Rev. B **51**, 2311 (1995).
 - ¹³J.-P. Schlomka, M. R. Fitzsimmons, R. Pynn, J. Stettner, O. H. Seeck, M. Tolan, and W. Press, Physica B **221**, 44 (1996).
 - ¹⁴J. Stettner, L. Schwalowsky, M. Tolan, O. H. Seeck, W. Press, C. Schwarz, and H. v. Känel, Phys. Rev. B **53**, 1398 (1996).
 - ¹⁵V. Nitz, M. Tolan, J.-P. Schlomka, O. H. Seeck, J. Stettner, W. Press, M. Stelzle, and E. Sackmann, Phys. Rev. B **54**, 5038 (1996).
 - ¹⁶A. L. Barabási, H. E. Stanley, *Fractal Concepts in Surface Growth* (Cambridge University Press, Cambridge, England, 1995).
 - ¹⁷C. Thompson, G. Palasantzas, Y. P. Feng, S. K. Sinha, and J. Krim, Phys. Rev. B **49**, 4902 (1994).
 - ¹⁸T. Salditt, T. H. Metzger, and J. Peisl, Phys. Rev. Lett. **73**, 2228 (1994).
 - ¹⁹S. F. Edwards and D. R. Wilkinson, Proc. R. Soc. London, Ser. A **381**, 17 (1982).
 - ²⁰F. Wu, S. G. Jaloviar, D. E. Savage, and M. G. Lagally, Phys. Rev. Lett. **71**, 4190 (1993).
 - ²¹P. E. Hegeman, H. J. W. Zandvliet, G. A. M. Kip, and A. van Silfhout, Surf. Sci. **311**, L655 (1994).
 - ²²T. Yoshinobu, A. Iwamoto, K. Sudoh, and H. Iwasaki, J. Vac. Sci. Technol. B **13**, 1630 (1995).
 - ²³P. Meakin, Phys. Rep. **235**, 189 (1993).
 - ²⁴M. F. Barnsley, R. L. Devaney, B. B. Mandelbrot, H.-O. Peitgen, D. Saupe, and R. F. Voss, *The Science of Fractal Images* (Springer-Verlag, Berlin, 1988).
 - ²⁵J. Krug and H. Spohn, in *Solids Far from Equilibrium: Growth Morphology and Defects*, edited by C. Godrèche (Cambridge University Press, Cambridge, England, 1991).
 - ²⁶F. Family and T. Vicsek, J. Phys. A **18**, L75 (1985).
 - ²⁷The KPZ equation cannot be formally derived. It is an expansion of the Edward-Wilkinson (EW) growth equation including a nonlinear term that takes into account that growth occurs perpendicular to the *local* surface. The EW equation is the lowest-order growth equation possible [besides the trivial $\partial s(\mathbf{r}, t)/\partial t = \eta(\mathbf{r}, t)$] that fulfills the symmetry requirements of a physical growth process (Ref. 16).
 - ²⁸The dimension n means the dimension of the substrate surface. Deposition of a film on a substrate is therefore a two-dimensional process.
 - ²⁹R. J. Temkin, G. A. N. Connell, and W. Paul, in *Amorphous and Liquid Semiconductors*, edited by J. Stuke and W. Brenig (Taylor & Francis, London, 1974).
 - ³⁰*Properties of Amorphous Silicon*, 2nd ed. (INSPEC, London, 1989), p. 471–472.
 - ³¹R. Kuschnerreit, H. Fath, A. A. Kolomenskii, M. Szabadi, and P. Hess, Appl. Phys. A **61**, 269 (1995).
 - ³²J. Shinar, H. Jia, R. Shinar, Y. Chen, and D. L. Williamson, Phys. Rev. B **50**, 7358 (1994).
 - ³³L. Brügemann, R. Bloch, W. Press, and M. Tolan, Acta Crystallogr. Sec. A **48**, 688 (1992).
 - ³⁴M. Tolan, D. Bahr, J. Süßenbach, W. Press, F. Brinkop, and J. P. Kotthaus, Physica B **198**, 55 (1994).
 - ³⁵For the 2000-Å film the vertical correlation could not be determined due to the limited resolution of the diffuse scattering experiment in the q_z direction.
 - ³⁶J. Krug, Adv. Phys. **46**, 139 (1997).
 - ³⁷F. König, Ph.D. thesis, ISI Forschungszentrum Jülich GmbH, 1995.